12-19-2020

Traveling-Wave Electrophoresis: 1D Model

Austin Green
Utah State University

Traveling-wave electrophoresis: 1D model

Austin Green, Mentor: Boyd F. Edwards
Department of Physics
Utah State University
Logan, UT 84322
(Dated: December 19, 2020)

A 1D model of traveling-wave electrophoresis predicts that molecular diffusion raises the trapping threshold and that other physical properties of the species effect the trapping threshold as well. Small concentrations, below 5 μM, raise the trapping threshold for high diffusivity species, resulting in a lower efficiency. Species with a mid-range electrophoretic mobility and diffusivity have their trapping threshold slightly lowered with an increase in concentration, leading to more particles traveling with the wave.

BACKGROUND

Traveling-wave electrophoresis is a microfluid technique used for separating ions and other charged particles based on their electrophoretic mobilities. The aim of traveling-wave electrophoresis is to use such a traveling wave to selectively transport charged species through a stationary, neutral fluid. The traditional physical design for traveling-wave electrophoresis uses an applied oscillating potential with electrodes embedded in the channel walls. This model then drives the electrons along the channel [1–3]. A sandwich architecture with electrodes both above and below the microfluidic channel has been introduced to avoid the need for static gravitational or electric fields [4].

The purpose of this paper is to investigate the effect different physical properties have on the trapping threshold, the ability for a particular species to be trapped by the wave and carried along the channel or immobilized at a particular region of the channel. Some of the properties I am particularly interested in studying is molecular diffusion and species concentration. By considering a simple 1D model I can understand the basic physics of traveling-wave electrophoresis. With this simple model, I can isolate and evaluate the role the physical properties have in raising or lowering the trapping threshold.

Molecular diffusion is vital to understanding a related technique called capillary electrophoresis. With capillary electrophoresis a static electric field is used instead of a traveling wave to separate charged species based on their electrophoretic mobilities. As bands of different charged species begin to appear, molecular diffusion will cause the bands to spread and the resolution of the separation worsens.

Some of the advantages of traveling-wave electrophoresis over capillary electrophoresis is the sharpness and tunability of the trapping threshold. Molecular diffusion might soften the sharpness of the trapping threshold while it is not expected to influence the tunability of the threshold, since the tunability relies only on changing the frequency of the wave. With capillary electrophoresis anions and cations travel in different directions while cations and anions travel in the same direction in traveling-wave electrophoresis. Another advantage of traveling-wave electrophoresis is the low voltage needed to produce the phenomenon, typically from 0.5 to -0.5 V. This low voltage decreases the size of the system enabling it to be put on a simple computer chip and powered with a cell phone battery.

The names and values for the symbols in the Model section are given in the following table.

Symbol	Name
$\phi(x,t)$	Potential
$n_l(x,t)$	Species Number Density
$\mathbf{j}_l(x,t)$	Species Flux Density
λ	Wavelength
ρ	Charge Density
e	Electronic Charge
z_l	Integer Valence
$\bar{n}$	Average Number Density for Cations
$\bar{n}_l$	Average Number Density for a Species
ϵ	Permittivity of Fluid
c	Wave Speed
μ_l	Electrophoretic Mobility
D_l	Diffusivity of the Species
ϕ_0	Magnitude of Applied Potential
E_0	Magnitude of Applied Electric Field
$\bar{n}_l$	Average Number Density for a Species
ϕ'	Dimensional Applied Potential
ψ'	Dimensionless Potential from Charged Species
$\mathbf{j}'_l$	Dimensional Species Flux Density
n'_l	Dimensional Species Number Density
S	Screening Number
R_l	Species Responsiveness Number
P_l	Species Péclet Number
$\bar{u}_l$	Average Species Speed

TABLE I: Name of the symbols that occur in the Model Section of the paper. The table serves as a handy reference to what everything is.

MODEL

There are three functions, the potential $\phi(x,t)$, the species number density $n_l(x,t)$, and the species flux den-

sity $\mathbf{j}_l(x,t)$ over the region $-\lambda/2 < x < \lambda/2$ where λ is the wavelength of the wave, that I am interested in modeling. The functions are defined to be periodic such that they satisfy $\phi(x+\lambda,t) = \phi(x,t)$, $\mathbf{j}_l(x+\lambda,t) = \mathbf{j}_l(x,t)$, and $n_l(x+\lambda,t) = n_l(x,t)$.

In the 1D model, a traveling wave is created by a periodic array of planar electrodes that move along the chanel at a constant speed c with respect to the stationary fluid. These electrodes are held at constant potentials of alternating sign, ϕ_0 and $-\phi_0$, with each pair of electrodes separated by a distance of $\lambda/2$. If the region between planes is electroneutral, then the resulting potential is a triangle wave of amplitude ϕ_0 and wavelength λ that propagates at speed c. Accordingly, the moving electrodes are consider to be porous, like wire mesh screens, to allow fluid to flow through the moving electrodes.

It is helpful to move into a co-moving reference frame from the laboratory reference frame in which the electrodes appear to be stationary and the background fluid and species flux density move in the $-\mathbf{x}$ direction except for the particles that are trapped with the wave, for which $\mathbf{j}_l(x,t) = 0$.

In this co-moving frame the functions evolve according to three differential equations.

$$\frac{\partial^2 \phi}{\partial x^2} = -\frac{e}{\epsilon}\sum_{l=1}^{N} z_l n_l \tag{1}$$

$$j_l = -c n_l - \mu_l n_l \frac{\partial \phi}{\partial x} - D_l \frac{\partial n_l}{\partial x} \tag{2}$$

$$\frac{\partial n_l}{\partial t} = -\frac{\partial j_l}{\partial x}. \tag{3}$$

Here Equation (1) is Poisson's Equation relating the potential and the species number density. Equation (2) is the Nernst-Planck flux density and it accounts for advection, electrophoresis, and diffusion. Equation (3) is the Continuity Equation and implies the conservation of species.

These functions are subject to the conditions

$$\phi(x,t) = -\phi_0 \tag{4}$$

at $x = 0, \pm\lambda, \pm 2\lambda, \ldots$ and

$$\phi(x,t) = \phi_0 \tag{5}$$

for $x = \pm\lambda/2, \pm 3\lambda/2, \ldots$, since the potential needs to alternate signs with every electrode. The condition

$$\bar{n}_l = \lambda^{-1}\int_{-\lambda/2}^{+\lambda/2} n_l(x,t)dx \tag{6}$$

implies that there must be some uniform average species number density throughout time, reflecting conservation of species.

Faradaic reactions permit electron exchange between the electrodes and the conducting solution, preventing charge accumulation at electrodes and facilitating an electroneutral solution with a vanishing global charge density

$$\int_{-\lambda/2}^{+\lambda/2} \rho dx = 0 \tag{7}$$

Where the charge density is

$$\rho = e\sum_{l=1}^{N} z_l n_l \tag{8}$$

and e, z_l are the electronic charge and integer valence number respectively. Dividing Equation (8) by e and considering only the positive charges yields

$$\bar{n} = \sum_{\text{cations}} z_l \bar{n}_l, \tag{9}$$

which is a useful measure of the concentration of the cations in the solution.

I am particularly interested in the steady-state charged distributions, which are reached in the limit $t \to \infty$. In this limit, the time derivative in Equation (3) is zero and integrating the equation requires there to be a uniform species flux density. By considering the steady-state charge distribution the species flux density takes on the form

$$j_l = -\left(c - \bar{u}_l\right)\bar{n}_l, \tag{10}$$

where $\bar{u}_l$ is the average speed of ions for species l.

The functions are then non-dimensionalized, the benefit of doing so allows the physical constants to be gathered into dimensionless variables making it easier to see how they influence the dynamics. The functions are assumed to have the form

$$\phi(x,t) = \phi_0\left[\phi'(2x/\lambda) + \psi'(2x/\lambda, 2ct/\lambda)\right] \tag{11}$$

$$j_l(x,t) = c\bar{n} j_l'(2x/\lambda, 2ct/\lambda) \tag{12}$$

$$n_l(x,t) = \bar{n} n_l'(2x/\lambda, 2ct/\lambda). \tag{13}$$

$$\phi'(x') = -1 + 2|x'| \tag{14}$$

where they depend on the dimensionless variables $x' = 2x/\lambda$ and $t' = 2ct/\lambda$. The potential in Equation (11) has been defined in two parts, an applied triangular-wave potential ϕ' and the potential from the redistribution of the charged species ψ'. Equations (11)-(14) are then substituted into Equations (1),(2), and (10) and the physical variables are gathered into dimensionless variables.

$$\frac{d^2\psi'^{(\pm)}}{dx'^2} = -2S\sum_{l=1}^{N} z_l n_l'^{(\pm)} \tag{15}$$

$$\frac{1}{P_l}\frac{dn_l'^{(\pm)}}{dx'} + \left(1 \pm R_l + \frac{R_l}{2}\frac{d\psi'^{(\pm)}}{dx'}\right) n_l'^{(\pm)} = -j_i', \tag{16}$$

$$j_l' = -\left(1 - \frac{\bar{u}_l}{c}\right)\frac{\bar{n}_l'}{\bar{n}}. \tag{17}$$

Here the dimensionless potential from the redistribution of the charged species and the dimensionless species number density are defined in a piece-wise manner

$$\psi'(x') = \begin{Bmatrix} \psi'^{(+)}(x') & 0 < x' < 1 \\ \psi'^{(-)}(x') & -1 < x < 0 \end{Bmatrix} \tag{18}$$

$$n_l'(x') = \begin{Bmatrix} n_l'^{(+)}(x') & 0 < x' < 1 \\ n_l'^{(-)}(x') & -1 < x' < 0 \end{Bmatrix}. \tag{19}$$

where the region from $-1 < x < 0$ is denoted with $(-)$ and the region from $0 < x < 1$ is denoted with $(+)$. Because of this piece-wise definition there must be matching conditions

$$n_l'^{(+)}(0) = n_l'^{(-)}(0) \tag{20}$$

$$n_l'^{(+)}(1) = n_l'^{(-)}(-1), \tag{21}$$

on the species number density to ensure the function is continuous across the two regions.

The boundary conditions on the potential become

$$\psi'^{(\pm)}(0) = \psi'^{(\pm)}(\pm 1) = 0, \tag{22}$$

since the species and the electrode can't be in the same physical location in one dimension.

The conservation condition becomes

$$\frac{\bar{n}_l}{\bar{n}} = \frac{1}{2}\int_{-1}^{0} n_l'^{(-)}(x')dx' + \frac{1}{2}\int_{0}^{+1} n_l'^{(+)}(x')dx'. \tag{23}$$

where $\bar{n}_l/\bar{n}$ is the ratio of the average species number density to the average number density for cations. For a system with 2 species the ratio is 1.

Three dimensionless numbers govern the dynamics. The screening number

$$S = \frac{e\lambda\bar{n}}{2\epsilon E_0} \tag{24}$$

measures the availability of charge to screen the electrode potentials, being dependent on the average number density $\bar{n}$ of positive charges. In effect, it is a measure of the concentration of the cation in the solution.

The responsiveness

$$R_l = \frac{\mu_l E_0}{c} \tag{25}$$

is the ratio of the average electrophoretic velocity of species l to the wave speed, and is positive for cations and negative for anions.

The mass transfer Péclet number

$$P_l = \frac{\lambda c}{2D_l} \tag{26}$$

measures the relative importance of diffusion for species l.

METHOD

Equations (15) and (16) imply a non-linear, coupled set of differential equations. Analytical methods of solving these equation have proven to be difficult. A numerical approach could be an easier way to approximate the solutions to the differential equations. Here I used both a forwards and backwards finite difference, discretizing the n_l' and ψ' functions and their derivatives. I discretized the functions into 401 nodes with the distance between each node being $d = 0.005$.

The benefit of doing so is that discretizing the functions and equations results in a set of unknown variables and a set of equations to solve for them. I used Scipy's function "fsolve" in a python program to solve the set of non-linear equations. I used a discretized version of the matching and average conditions given in Equations (20)-(23) to help solve for the unknowns. I used a trapezoid rule approximation to discretize the integrals in Equation (23). I then averaged the two results together, in effect simulating what a centered finite difference would be.

The ratio $\bar{u}_l/c$ in Equation (17) is the ratio of the charged ions speed to the wave speed c. This ratio can be calculated by using the approximated species flux density that is found from discretizing. Values closer to one means that the species is trapped with the wave and travels with it while lower values indicate the species lags behind the wave. By calculating this value I can discover how changing the physical properties of a species influences the trapping threshold.

In the following numerical approximations only two species were considered. The species were considered to have the same physical properties except they had opposite charges, namely one was an anion and one was a cation. The benefit in doing so results in the speed of the charged species to be the same, allowing me to report one value. Another benefit of a two species system is that the Screening number, S, is proportional to the concentration of the system since there must be the same amount of anion and cation in the solution. Different physical properties were tested by adjusting S, R_l, P_l, the Screening,

Responsiveness, and Péclet numbers respectively. Except for the concentration of the charged species, only the physical values for the species was changed, all other values were held constant for every approximation.

RESULTS

Symbol	Value
e	$1.6 \times 10^{-19}\ C$
λ	$80\mu m$
$\bar{n}$	6.02×10^{18}
ϵ	$80 \times 8.85 \times 10^{-12} C/Vm$
E_0	25000V/m
c	80×10^{-6}m/s

TABLE II: These values are held constant for every approximation except for $\bar{n}$ which is changed to reflect different concentration amounts.

Table II shows the physical values of the system, such as wavelength and wave speed. The value for $\bar{n}$ is calculated by multiplying Avogadro's number and a standard molar concentration of 10 μM. The value for S was then calculated to be $S = 2177$. There were five different approximations corresponding to five different S values, one at the original concentration, one at half the original concentration when $S = 1089$, one at 75% of the original concentration when $S = 1698$, one at double the initial concentration when $S = 4354$, and when $S = 0$. $S = 0$ corresponds to when species concentration is low enough that it doesn't influence the charge redistribution potential. The species velocity was then graphed for each S value and for several different R_l and P_l values in increments of 0.25.

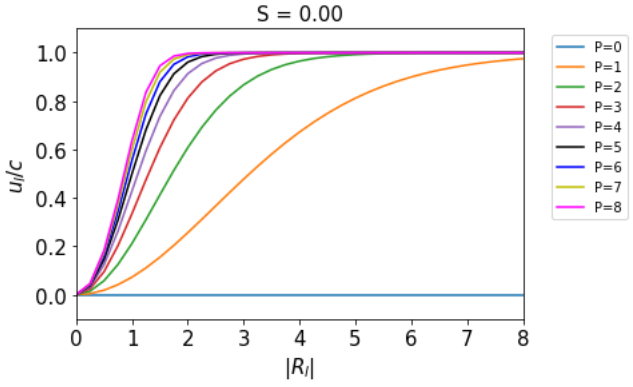

FIG. 1: Ratio of steady-state average ion velocity $\bar{u}$ to wave speed c as a function of mobility number $|R|$ for $S = 0$ and for Péclet numbers $P = 0$, 1, 2, 3, 4, 5, 6, 7, and 8. Values closer to 1 means the particle travels with the wave better.

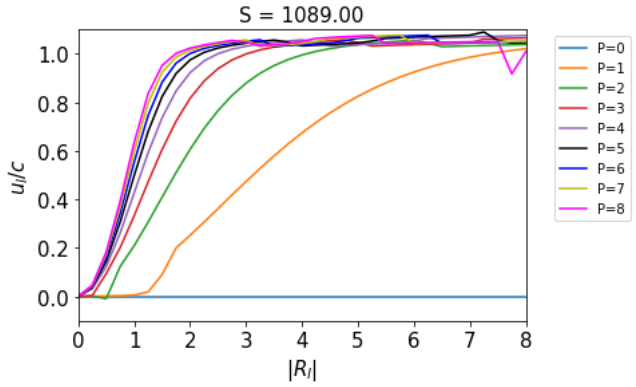

FIG. 2: Ratio of steady-state average ion velocity $\bar{u}$ to wave speed c as a function of mobility number $|R|$ for $S = 1089$ and for Péclet numbers $P = 0$, 1, 2, 3, 4, 5, 6, 7, and 8. Values closer to 1 means the particle travels with the wave better.

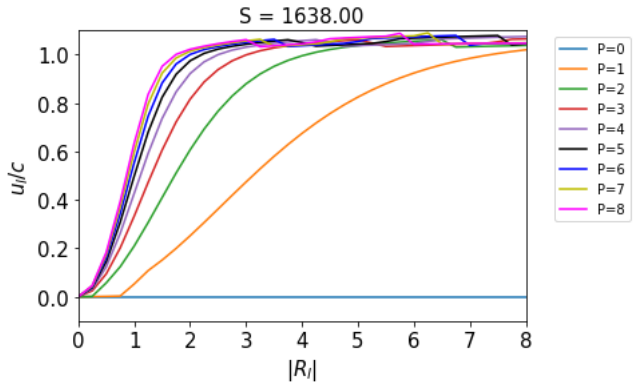

FIG. 3: Ratio of steady-state average ion velocity $\bar{u}$ to wave speed c as a function of mobility number $|R|$ for $S = 1638$ and for Péclet numbers $P = 0$, 1, 2, 3, 4, 5, 6, 7, and 8. Values closer to 1 means the particle travels with the wave better.

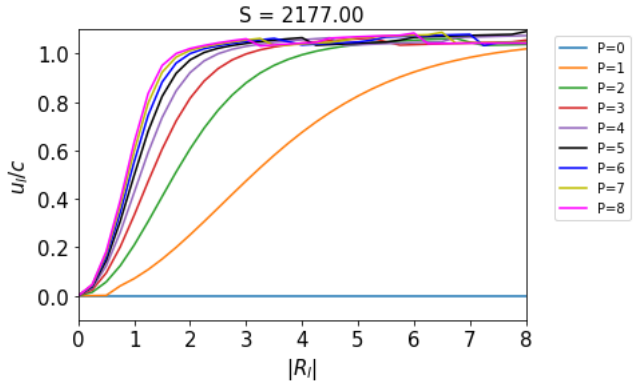

FIG. 4: Ratio of steady-state average ion velocity $\bar{u}$ to wave speed c as a function of mobility number $|R|$ for $S = 2177$ and for Péclet numbers $P = 0$, 1, 2, 3, 4, 5, 6, 7, and 8. Values closer to 1 means the particle travels with the wave better.

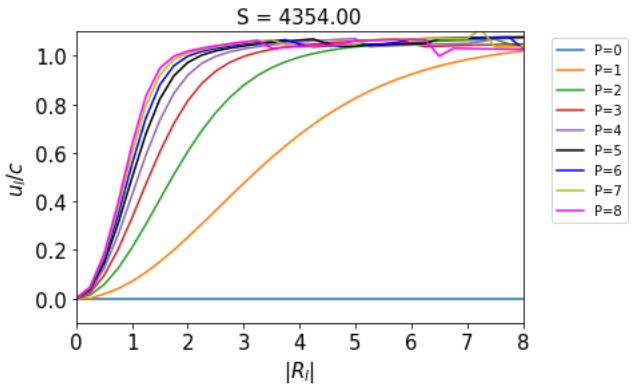

FIG. 5: Ratio of steady-state average ion velocity $\bar{u}$ to wave speed c as a function of mobility number $|R|$ for $S = 4354$ and for Péclet numbers $P = 0$, 1, 2, 3, 4, 5, 6, 7, and 8. Values closer to 1 means the particle travels with the wave better.

DISCUSSION

We see that for the $S = 0$ graph, which reflects a small concentration, the particles with low P_l (high diffusivity) and low R_l (low electrophoretic mobilities) values struggle to stay with the wave. However for P_l values greater than 1, we see that the trapping threshold is lowered, resulting in species traveling with the wave. It's also clear that for P_l values greater than 5 and R_l values greater than 2 most particles are trapped with the wave.

Curiously, with small enough concentrations the trapping threshold is raised for small R_l and P_l values. Having a species that struggles to keep with the wave and then adding more of that species seems to have a negative effect. It appears that the reverse is true for R_l and P_l values from 3 to 6. There is a slight decrease in the trapping threshold, resulting in more species particles traveling with the wave.

As the concentration amount is increased the approximation becomes less accurate for higher R_l and P_l values. One way to decrease this inaccuracy is by increasing the amount of nodes when discretizing. However, time restraints prevented me from doing so. However the general trend still seems to show that larger P_l and R_l values result in particles traveling with the wave. It's also apparent that concentrations above 5 μM helps lower R_l and P_l values stay with the wave.

In conclusion, it seems that the results agree with the theory that molecular diffusion plays a significant role with influencing the trapping threshold. In particular, species with low P_l (high diffusivity) and low R_l (electrophoretic mobilities) values have trouble staying with the wave, which is further amplified with a small increase in concentration. However the trapping threshold can be reduced for these small values by increasing the concentration to around 7.5 μM or greater. For species with sufficiently high P_l (low diffusivity) and R_l values (electrophorectic mobilities) the concentration didn't seem to have much of an effect. These results also strengthen the idea that a simple 1D model can work to show insight into traveling-wave electrophoresis.

[1] S. Masuda, M. Washizu, and M. Iwadare, IEEE Trans. Ind. Appl. **IA-23**, 474 (1987).

[2] H. Kawamoto and S. Hayashi, J. Phys. D **39**, 418 (2006); H. Kawamoto, K. Seki, and N. Kuromiya, J. Phys. D **39**, 1249 (2006), and references therein.

[3] M. H. Lean, H. B. Hsieh, A. R. Volkel, IEEE/EMBS Proc. Conf. on Microtechnologies in Medicine and Biology, 356 (2005); M. H. Lean, H. B. Hsieh, J.-P. Lu, J. H. Daniel, B. T. Preas, and S. J. Limb, ibid., p. 80.

[4] B. F. Edwards, A. T. Timperman, R. L. Carroll, K. Jo, J. M. Mease, and J. E. Schiffbauer, Phys. Rev. Lett. **102**, 076103 (2009).